

RESEARCH ARTICLE

Diabetes-Associated Changes in the Toe Photoplethysmogram During Local Heating Test

Denis Lapitan¹  | Xiaoman Xing^{2,3} | Alexey Glazkov¹ | Ksenia Krasulina¹ | Yulia Kovaleva¹ | Polina Glazkova¹ | Timur Britvin¹ | Sergey Zagarov¹ | Roman Larkov¹ | Dmitry Rogatkin¹

¹Moscow Regional Research and Clinical Institute (“MONIKI”), Moscow, Russia | ²Division of Life Sciences and Medicine, School of Biomedical Engineering (Suzhou), University of Science and Technology of China, Suzhou, China | ³Suzhou Institute of Biomedical Engineering and Technology, Chinese Academy of Sciences, Suzhou, China

Correspondence: Denis Lapitan (lapitandenis@mail.ru)

Received: 19 April 2025 | **Revised:** 27 June 2025 | **Accepted:** 16 July 2025

Funding: The authors received no specific funding for this work.

Keywords: diabetes mellitus | endothelial regulation | heating test | neurogenic regulation | photoplethysmography | pulse waveform

ABSTRACT

We investigated changes in the pulse waveform recorded by photoplethysmography (PPG) during a local heating test in patients with diabetes. The following groups of subjects were studied: healthy individuals ($n=15$), patients with Type 2 diabetes accompanied by diabetic retinopathy ($n=14$), patients with Type 2 diabetes and diabetic foot syndrome ($n=16$). Measurements were taken from the big toes of both limbs while the skin was heated from 32°C to 42°C. We found statistically significant changes in PPG waveform after heating between all three groups. The main change is that the dicrotic notch becomes more pronounced during the heating period. This effect is strongest in Group 1, slightly less pronounced in Group 2, and practically absent in Group 3. Thus, monitoring of the PPG waveform during the heating test may be an effective means of assessing microvascular lesions in diabetes.

1 | Introduction

The number of people with diabetes mellitus (DM) has increased four times in the last 30 years and exceeded 800 million [1]. DM, particularly, Type 2 diabetes, is associated with chronic hyperglycemia, which leads to endothelial dysfunction, oxidative stress, and inflammation, all of which impair microvascular and macrovascular systems [2]. Researchers use various optical techniques to evaluate microvascular lesions in DM, such as capillaroscopy, laser Doppler flowmetry, laser speckle contrast imaging, diffuse reflectance spectroscopy, and so forth [3–5]. One of the most technically simple techniques is photoplethysmography (PPG), which is based on the illumination of a tissue with incoherent optical radiation in the visible or near-infrared range and recording a signal that has passed through or backscattered from the tissue [6]. This method allows for recording the pulse wave propagating

through the vascular bed of the tissue. Morphological analysis of the PPG waveform provides important information about the state of blood vessels, for example, their stiffness, tone, compliance, and so forth [7, 8].

There are quite a lot of methods for detecting vascular lesions in DM using PPG. We can distinguish traditional methods based on the analysis of the variable (AC) and slowly changing (DC) components of the PPG signal, heart rate variability, the first and second derivatives of the signal, and so forth, machine learning methods such as support vector machine, decision tree, and so forth, and deep learning methods (mainly convolutional neural networks) [9]. For example, Pilt et al. assessed the validity of the PPG waveform augmentation index (PPGAI) for the estimation of increased arterial stiffness on healthy subjects and Type 2 DM patients [10]. This index revealed a significant difference between the groups of diabetes

patients and healthy controls and can be considered as a perspective measure of increased arterial stiffness estimation in clinical screenings. Reddy et al. developed an application for processing finger PPG signals that gave 80% specificity and 84% sensitivity in detecting diabetes for a 100-patient dataset [11]. Nirala et al. used characteristic features of toe photoplethysmogram for the detection of Type 2 DM using support vector machine [12]. Using a 10 selected features set, they gained an accuracy of 97.87%, sensitivity of 98.78%, and specificity of 96.61%.

However, in the mentioned works, the signals are usually recorded in a calm state of the subject without functional influences. Meanwhile, the results of the use of functional tests on the microcirculatory bed are often more reproducible compared to the results at rest [13, 14]. Kamshilin et al. used local thermal impact for assessment of parameters of the cutaneous blood flow during thermoregulation by imaging PPG system [15]. Their experiments show that the blood pulsation amplitude is a sufficiently reliable index, which could characterize the relative change of the cutaneous blood flow. However, in this study, the authors did not examine changes in pulse waveform after skin heating.

Local heat testing has been shown to be highly informative in patients with DM. The local thermal hyperaemia methodology may become a valuable noninvasive tool for diagnosis and assessing progress of diabetes-related microvascular complications [16]. For example, Mizeva et al. used a local heating test in conjunction with laser Doppler flowmetry to assess the state of the microvascular bed in Types 1 and 2 diabetes [17]. Their study demonstrated that the diabetic patients have impaired vasodilation in response to heating. The benefits of local heating are due to its ability to assess both endothelial and neurogenic components of vasodilation [18, 19], providing quantitative measurements suitable for monitoring disease progression and response to treatment. The impaired vasodilatory response to local heating observed in diabetic patients reflects underlying endothelial dysfunction, impaired neurogenic regulation, and structural vascular changes that collectively reflect the increased cardiovascular risks associated with diabetes.

The aim of this work is to investigate changes in the PPG waveform during local heating test in healthy subjects and patients with Type 2 DM.

2 | Materials and Methods

2.1 | Subjects

The study included three groups of patients. Group 1 included healthy individuals without any disturbances in carbohydrate metabolism. Group 2 included patients diagnosed with Type 2 DM accompanied by diabetic retinopathy. Group 3 consisted of patients with Type 2 DM who also exhibited diabetic foot syndrome or peripheral arterial disease.

The inclusion criteria for Group 1 (healthy volunteers) were as follows:

- aged between 18 and 44 years,
- absence of any carbohydrate metabolism disorders,
- no history of cardiovascular or pulmonary diseases,
- body mass index (BMI) below 25 kg/m^2 .

For Group 2, the criteria included as follows:

- age range of 45–74 years,
- a confirmed diagnosis of Type 2 DM,
- presence of peripheral neuropathy and retinopathy (non-proliferative or preproliferative stages),
- ongoing antidiabetic treatment, including insulin therapy, for a minimum of 3 months,
- no prior cardiovascular incidents (such as myocardial infarction, stroke, or coronary/carotid revascularization),
- absence of diabetic foot syndrome and peripheral arterial disease.

Group 3 inclusion criteria were as follows:

- age 45–74 years,
- confirmed type 2 DM diagnosis,
- presence of either diabetic foot syndrome or peripheral arterial disease.

Exclusion criteria applicable to all groups were: diagnosis of any malignancy within the preceding 5 years, systemic autoimmune diseases, severe cardiac arrhythmias (e.g., atrial fibrillation, frequent extrasystoles), acute viral infections, fever of any origin (body temperature exceeding 37.0°C), acute exacerbation of chronic conditions, hematologic disorders (e.g., thrombocytopenia, anemia), dermatologic conditions that could interfere with the study, history of vascular thrombosis, elevated thrombosis risk, pregnancy, end-stage chronic kidney disease (Stage 5), ongoing use of nonsteroidal anti-inflammatory drugs, hormonal or contraceptive medications, inability to independently attend or complete the study procedures, and any other conditions deemed by the investigators to potentially influence the study outcomes.

All participants provided informed consent before enrollment. The study adhered to the ethical guidelines outlined in the Declaration of Helsinki (2013 revision) and received approval from the Independent Ethics Committee of the Moscow Regional Research and Clinical Institute (Protocol No. 13, dated November 7, 2019).

A total of 45 subjects were included in the study, and the clinical characteristics of the subjects are shown in Table 1.

2.2 | Acquisition of PPG Signals

PPG data were collected using a self-made automated device for studying central and peripheral hemodynamics [20]. The device consists of a standard tonometer cuff and three

optical sensors attached to the subject's limb. The optical sensors use three green LEDs (FYL-3014UGC, Ningbo Foryard Optoelectronics Co., China) with a peak emission wavelength of 568 nm to illuminate the tissue and one silicone photodiode (SFH 229, Osram Opto Semiconductors GmbH, Germany) to record the backscattered signal. The sensors also have a

built-in metal plate to heat the skin to the desired temperature. The appearance of the device and the attachment of the sensors to the big toes of the subject during measurements are shown in Figure 1. Raw PPG signals were recorded at a sampling rate of 320 Hz and saved to a computer for further processing.

TABLE 1 | Clinical characteristics of the subjects.

Parameter	Group			Pairwise comparisons
	1, n = 15	2, n = 14	3, n = 16	
Age, years, Me [LQ; UQ]	25 [22.5; 30.5]	57 [50.2; 62.2]	64.5 [58.2; 70.5]	1–2: < 0.001*
Min–max	21–44	37–71	48–81	1–3: < 0.001*
				2–3: 0.163
Sex	Female, n (%)	9 (60%)	11 (78.6%)	1–2: 0.497
	Male, n (%)	6 (40%)	3 (21.4%)	1–3: 0.425
				2–3: 0.078
BMI, kg/m ² , Me [LQ; UQ]	21.8 [19.7; 23.8]	32.6 [28.3; 35.1]	28.2 [25.7; 33.4]	1–2: < 0.001*
Min–max	16.8–25.0	22.3–41.1	22.7–35.1	1–3: < 0.001*
				2–3: 0.205
Arterial hypertension	No, n (%)	15 (100%)	4 (28.6%)	1–2: < 0.001*
	Yes, n (%)	0 (0%)	10 (71.4%)	1–3: < 0.001*
				2–3: 0.079
HbA1c, %, Me [LQ; UQ]	5.2 [5.1; 5.6]	9.2 [7.4; 10.1]	8.0 [7; 8.9]	1–2: < 0.001*
Min–max	5.0–5.7	6.4–12.2	5.8–10.9	1–3: < 0.001*
				2–3: 0.351
Retinopathy	No, n (%)	15 (100%)	5 (35.7%)	1–2: < 0.001*
	Yes, n (%)	0 (0%)	9 (64.3%)	1–3: 0.087
				2–3: 0.141
MNSI score, Me [LQ; UQ]	0 [0; 0]	13 [10.9; 14]	17 [14.2; 18.2]	1–2: < 0.001*
Min–max	0–1	7–16	8–19	1–3: < 0.001*
				2–3: 0.035*
NSS score, Me [LQ; UQ]	0 [0; 0]	7.5 [7; 8]	7.5 [7; 8]	1–2: < 0.001*
Min–max	0–0	7–8	6–9	1–3: < 0.001*
				2–3: 1

Note: In the “pairwise comparisons” column, *p* values are given for Dunn's test (quantitative data) or Fisher's exact test (qualitative data) with the Holm–Bonferroni correction.

**p* < 0.05.



FIGURE 1 | Photographs of the device used (a) and the attachment of the sensors to the subject's big toes during measurements (b).

In this article, we analyzed only the readings obtained from the sensor, which was placed on the big toe. PPG signals were recorded during the local heating tests. First, the values of indices in the baseline period (sensor temperature 32.2°C) were recorded for 40s; after measuring the pressure on the hand and a pause period, the sensor was rapidly heated to 42°C (approximately 2°C/s). The indices for the heating period were calculated for a period of 120–180s from the moment the heating was turned on.

2.3 | Signal Processing and Morphological Features

To enhance PPG signal quality, we applied a median filter with a window size of 5 to remove short-term artifacts while preserving waveform characteristics. This was followed by wavelet denoising using a Symlets wavelet at decomposition level 10.

The morphological features were derived from the PPG signals. Initially, we normalized each pulse by height to a range of 0–1 and resampled each pulse to a length of 100 data points. This choice had no inherent meaning and can be adjusted to suit specific requirements. Subsequently, we utilized a decomposition technique to extract essential characteristics from each pulse, as shown in Figure 2. This technique involved decomposing each pulse into five Gaussian components, incorporating key attributes such as height, location, and dispersion of each component [21, 22]. These pulses correspond to the forward and reflected waves.

We opted for the use of five Gaussian fittings for two primary reasons. First, this approach yielded superior fitting results compared to decompositions using only three or four Gaussians. Second, the tight constraints on the peak amplitudes and timing of the Gaussian components enabled clearer physiological interpretations. For ease of labeling, we designated the locations of Gaussians as b_{1-5} , the peaks as a_{1-5} , and the standard deviation as c_{1-5} in this study.

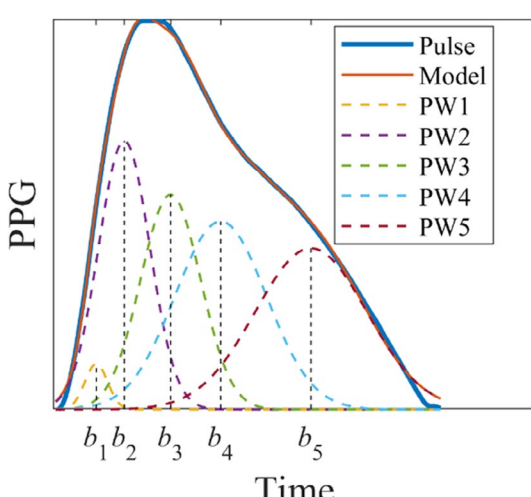


FIGURE 2 | Multi-Gaussian decomposition of PPG waveform. The center locations of pulse waves (PW) were denoted as b_{1-5} .

Next, we used the following features of the first derivative of the PPG signal due to their physiological meaning [23]:

- SPMAX—maximum of normalized first derivative in the systolic phase;
- SPMEAN—mean of normalized first derivative in the systolic phase;
- SPVAR—variance of normalized first derivative in the systolic phase;
- DPMEAN—mean of normalized first derivative in the diastolic phase;
- DPVAR—variance of normalized first derivative in the diastolic phase.

We also assessed the duration of the systolic period (SP), diastolic period (DP) and their ratio: DP/SP. In this study, SP is defined as the time from the valley of the PW to the systolic peak, and DP is defined as the time from the systolic peak to the next valley. In our previous study, we showed that the DP/SP index can serve as an indicator of peripheral vascular elasticity [24].

2.4 | Statistical Analysis

Statistical analysis was performed in RStudio 2024.12.0 (Posit Software, PBC) using R language version 4.3.3. Medians and quartiles (Me [LQ; UQ]), minimum–maximum (min–max) were calculated for quantitative variables. Quantitative variables in the three groups were compared using the Kruskal–Wallis (K-W) test with post hoc pairwise comparisons by Dunn's test. Differences in indices between the baseline period and the heating period were assessed using the paired Wilcoxon test. Qualitative data were compared using Fisher's exact test. The Holm–Bonferroni correction was applied for pairwise comparisons. The diagnostic informativeness of the different indices was evaluated using ROC analysis: the area under the ROC curve (AUC) with two-sided 95% confidence intervals was calculated. The Type-I error rate (α) was set to be 0.05. The null hypotheses were rejected when $p < \alpha$.

3 | Results

A total of 90 photoplethysmograms were analyzed (two for each patient—from the right and left limbs). In patients from Group 3, 10 limbs had signals with low amplitude of pulse oscillations (less than 20 mV), which made it difficult to identify specific pulse waves and calculate indices. Therefore, we excluded these 10 records from the final analysis. Examples of “normal amplitude” and “low amplitude” signals are shown in Figure 3.

Averaged plots for the period of registration of the baseline perfusion level and for the period of the heating were created (Figure 4). In all three groups, we see a leftward shift of the systolic peak during the heating period compared to the baseline period. Thus, heating leads to a more rapid rise of the systolic wave. By visual analysis, the shift value is the same

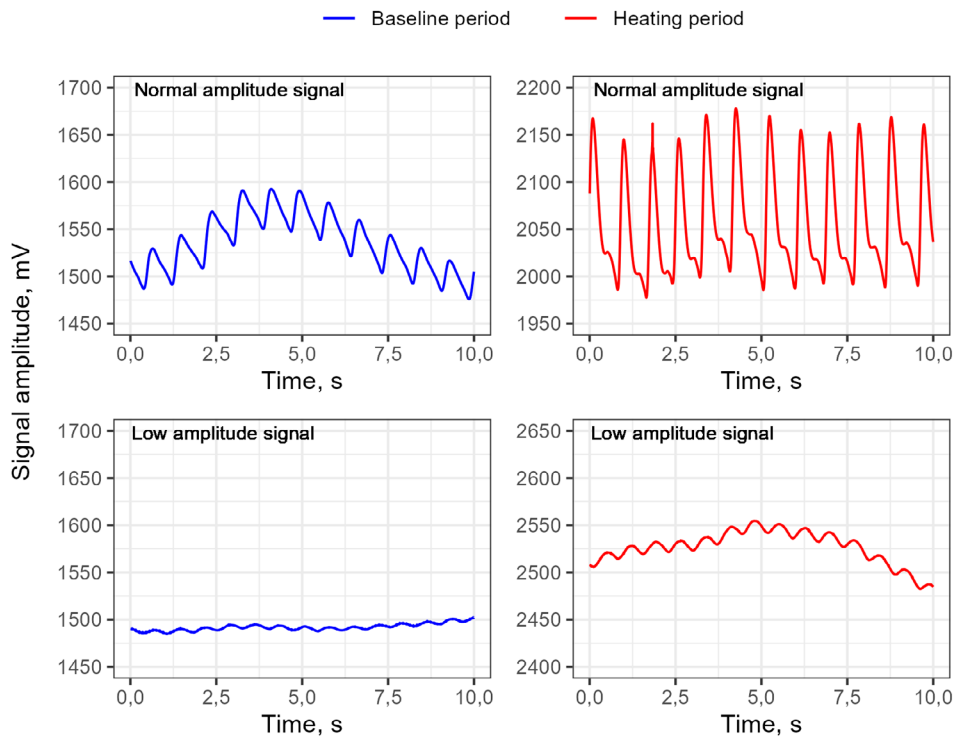


FIGURE 3 | Examples of PPG recordings with “normal” pulsatile amplitude and with “low” pulsatile amplitude at baseline and during the local heating test. The y axis spread in the plots is unified and equals 250 mV.

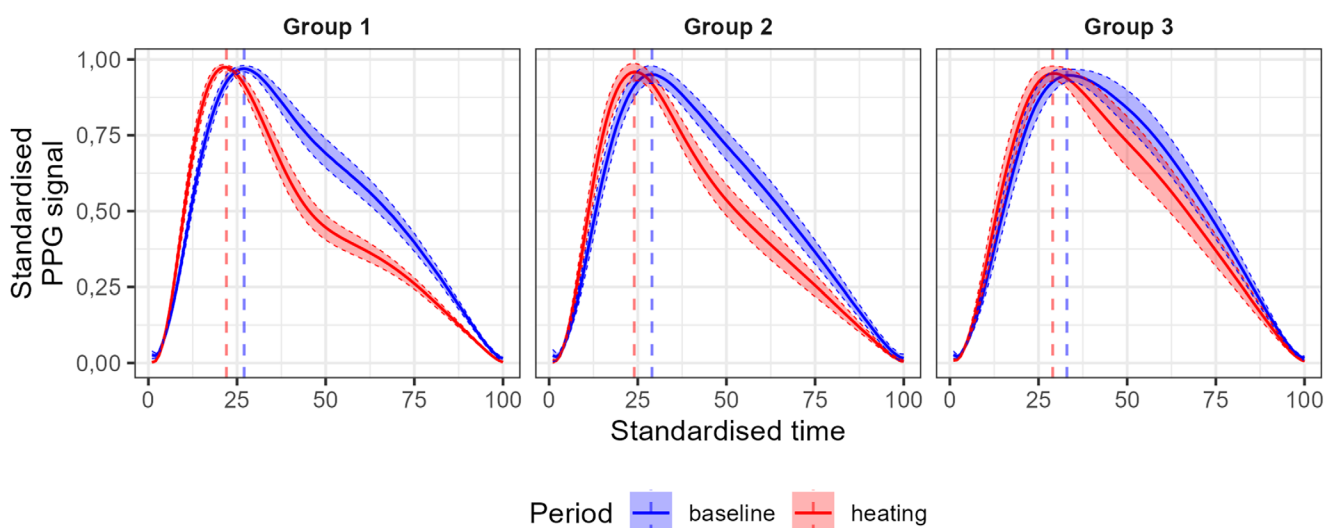


FIGURE 4 | Averaged standardized PPG signal in three groups of subjects during baseline and heating periods. Color-filled areas represent two-sided 95% confidence intervals.

across the groups. We also note an intensification of dicrotic notch curvature (lower amplitude of reflected wave, indicating lower peripheral resistance), and this effect is strongest in Group 1, slightly less pronounced in Group 2, and practically absent in Group 3.

We analyzed the main indices of the multi-Gaussian decomposition of the pulse waveform in the three groups (Table 2). We included in the final analysis only those indices that showed any differences (indices c_1 , c_3 , a_4 , a_5 , b_4 , b_5 , c_4 , c_5 were discarded). For each subject, indices were assessed on the left and right side of the body. The a_1 index differed in all three groups during the

baseline period. For the other indices, the K-W test also showed significant differences, but in pairwise comparisons, differences were not found between all groups.

Significant dynamics (baseline vs. heating) were observed for all indices except a_2 in all three groups. Index a_1 significantly increased, while indices a_3 , b_1 , b_2 , b_3 , and c_2 significantly decreased.

We also analyzed the indices of the first derivative and the temporal characteristics of the pulse waveform (Table 3). For all indicators except DP (both periods) K-W test showed statistically

TABLE 2 | Indexes of multi-Gaussian decomposition of PPG waveform in three groups of subjects (median [LQ; UQ] min–max).

Index	Period	Group			Pairwise comparisons
		1, n=30	2, n=28	3, n=22	
a_1	Baseline	0.123 [0.117; 0.135] 0.09–0.165	0.112 [0.102; 0.124] 0.08–0.183	0.094 [0.076; 0.1] 0.06–0.115	1–2: 0.037* 1–3: <0.001* 2–3: <0.001*
	Heating	0.146 [0.136; 0.167] 0.119–0.227***	0.135 [0.124; 0.153] 0.085–0.215***	0.093 [0.082; 0.107] 0.036–0.175+	1–2: 0.098 1–3: <0.001* 2–3: <0.001*
a_2	Baseline	0.593 [0.552; 0.615] 0.438–0.645	0.574 [0.548; 0.589] 0.47–0.621	0.556 [0.494; 0.586] 0.4–0.686	1–2: 0.177 1–3: 0.04* 2–3: 0.385
	Heating	0.568 [0.554; 0.605] 0.515–0.648	0.557 [0.531; 0.581] 0.49–0.631	0.547 [0.523; 0.564] 0.253–0.624	1–2: 0.043* 1–3: 0.011* 2–3: 0.454
a_3	Baseline	0.528 [0.5; 0.557] 0.453–0.586	0.511 [0.481; 0.545] 0.436–0.608	0.604 [0.53; 0.642] 0.473–0.805	1–2: 0.308 1–3: 0.007* 2–3: <0.001*
	Heating	0.482 [0.462; 0.512] 0.429–0.545***	0.484 [0.475; 0.498] 0.455–0.538++	0.521 [0.487; 0.61] 0.396–0.717***	1–2: 0.988 1–3: 0.005* 2–3: 0.005*
b_1	Baseline	0.119 [0.116; 0.124] 0.107–0.136	0.127 [0.118; 0.137] 0.098–0.154	0.138 [0.126; 0.151] 0.111–0.162	1–2: 0.057 1–3: <0.001* 2–3: 0.057
	Heating	0.107 [0.098; 0.118] 0.092–0.129***	0.114 [0.104; 0.128] 0.092–0.134***	0.123 [0.117; 0.131] 0.098–0.159***	1–2: 0.1 1–3: <0.001* 2–3: 0.1
b_2	Baseline	0.196 [0.186; 0.203] 0.164–0.225	0.205 [0.186; 0.219] 0.154–0.253	0.238 [0.215; 0.254] 0.183–0.264	1–2: 0.172 1–3: <0.001* 2–3: 0.005*
	Heating	0.164 [0.151; 0.185] 0.141–0.208***	0.178 [0.16; 0.199] 0.139–0.219***	0.216 [0.19; 0.229] 0.151–0.273***	1–2: 0.142 1–3: <0.001* 2–3: 0.003*
b_3	Baseline	0.316 [0.302; 0.335] 0.255–0.361	0.328 [0.29; 0.346] 0.239–0.399	0.379 [0.338; 0.419] 0.287–0.44	1–2: 0.707 1–3: <0.001* 2–3: <0.001*
	Heating	0.257 [0.229; 0.295] 0.217–0.336***	0.279 [0.249; 0.305] 0.223–0.329***	0.344 [0.298; 0.37] 0.226–0.447***	1–2: 0.27 1–3: <0.001* 2–3: 0.002*
c_2	Baseline	15.69 [14.91; 17.11] 12.11–18.26	16.36 [14.38; 16.93] 11.22–19.53	19.4 [16.52; 20.66] 14.17–22.21	1–2: 0.983 1–3: <0.001* 2–3: <0.001*
	Heating	12.44 [11.1; 14.47] 9.86–16.97***	13.43 [11.85; 14.72] 9.97–15.9***	17.69 [14.71; 18.87] 10.15–22.42***	1–2: 0.434 1–3: <0.001* 2–3: <0.001*

Note: In the “pairwise comparisons” column, p values are given for Dunn’s test with the Holm–Bonferroni correction only for variables for which the Kruskal–Wallis test showed a p value <0.05; in other cases, the p value for the K-W test is given.

*p<0.05 for Dunn’s test.

⁺p<0.05.

⁺⁺p<0.01.

***p<0.001 for Wilcoxon paired test (baseline vs. heating period comparison).

TABLE 3 | Features of the first derivative of the PPG signal, systolic and diastolic period durations (SP and DP), DP/SP ratio in three groups of subjects (median [LQ; UQ] min—max).

Index	Period	Group			Pairwise comparisons
		1, n=30	2, n=28	3, n=22	
SPMAX	Baseline	0.046 [0.042; 0.05] 0.035–0.063	0.042 [0.038; 0.048] 0.029–0.071	0.033 [0.03; 0.039] 0.024–0.047	1–2: 0.113 1–3: <0.001* 2–3: <0.001*
	Heating	0.059 [0.052; 0.064] 0.045–0.077***	0.053 [0.047; 0.061] 0.037–0.085***	0.036 [0.032; 0.043] 0.021–0.065***	1–2: 0.137 1–3: <0.001* 2–3: <0.001*
	Baseline	0.022 [0.02; 0.024] 0.016–0.03	0.021 [0.02; 0.024] 0.016–0.03	0.017 [0.015; 0.02] 0.013–0.024	1–2: 0.762 1–3: <0.001* 2–3: <0.001*
	Heating	0.029 [0.025; 0.032] 0.022–0.034***	0.025 [0.024; 0.028] 0.019–0.035***	0.02 [0.017; 0.023] 0.011–0.03***	1–2: 0.087 1–3: <0.001* 2–3: <0.001*
SPMEAN	Baseline	0.0146 [0.0132; 0.016] 0.0116–0.0203	0.0136 [0.0127; 0.0158] 0.0094–0.0224	0.0106 [0.0097; 0.0132] 0.0077–0.0152	1–2: 0.237 1–3: <0.001* 2–3: <0.001*
	Heating	0.0197 [0.0166; 0.0215] 0.0139–0.0247***	0.0176 [0.0154; 0.0197] 0.0124–0.0278***	0.012 [0.0108; 0.0145] 0.0058–0.0219***	1–2: 0.182 1–3: <0.001* 2–3: <0.001*
	Baseline	−0.008 [−0.0082; −0.0078] −0.0087–0.0076	−0.0083 [−0.0086; −0.008] −0.0097–0.0075	−0.0088 [−0.0092; −0.0085] −0.0109–0.0079	1–2: 0.018* 1–3: <0.001* 2–3: 0.013*
	Heating	−0.0076 [−0.008; −0.0074] −0.0082–0.0072***	−0.0079 [−0.0081; −0.0076] −0.0088–0.0074***	−0.0086 [−0.0092; −0.0081] −0.0104–0.0076**	1–2: 0.058 1–3: <0.001* 2–3: <0.001*
DPVAR	Baseline	0.0031 [0.0027; 0.0037] 0.0023–0.0056	0.003 [0.0024; 0.0032] 0.0021–0.0047	0.0034 [0.0029; 0.0043] 0.0019–0.006	1–2: 0.144 1–3: 0.432 2–3: 0.045*
	Heating	0.0051 [0.004; 0.0064] 0.0025–0.0091***	0.0046 [0.0034; 0.0051] 0.0023–0.0063***	0.0033 [0.0024; 0.0043] 0.002–0.0054	1–2: 0.07 1–3: <0.001* 2–3: 0.021*
	Baseline	0.241 [0.214; 0.265] 0.19–0.375	0.239 [0.224; 0.248] 0.208–0.312	0.307 [0.26; 0.347] 0.21–0.434	1–2: 0.9 1–3: <0.001* 2–3: <0.001*
	Heating	0.192 [0.179; 0.206] 0.162–0.239***	0.205 [0.193; 0.214] 0.174–0.251***	0.278 [0.222; 0.292] 0.187–0.395***	1–2: 0.173 1–3: <0.001* 2–3: <0.001*
DP	Baseline	0.658 [0.628; 0.702] 0.513–0.783	0.618 [0.508; 0.75] 0.39–0.936	0.626 [0.539; 0.708] 0.438–0.823	K-W test p=0.359
	Heating	0.689 [0.647; 0.749] 0.545–0.859***	0.66 [0.543; 0.79] 0.42–0.904***	0.639 [0.59; 0.734] 0.44–0.899***	K-W test p=0.288
DP/SP	Baseline	2.76 [2.52; 3.13] 2.09–3.89	2.51 [2.3; 3.01] 1.61–4.17	2.08 [1.66; 2.52] 1.41–3.05	1–2: 0.125 1–3: <0.001* 2–3: 0.009*
	Heating	3.7 [3.1; 4.07] 2.75–4.37***	3.19 [2.87; 3.72] 2.13–4.4***	2.4 [2.13; 2.85] 1.19–4.17***	1–2: 0.122 1–3: <0.001* 2–3: <0.001*

Note: In the “pairwise comparisons” column, p values are given for Dunn’s test with the Holm–Bonferroni correction only for variables for which the Kruskal–Wallis test (K-W test) showed a p value <0.05; in other cases, the p value for the K-W test is given.

*p<0.05 for Dunn’s test.

**p<0.01.

***p<0.001 for Wilcoxon paired test (baseline vs. heating period comparison).

significant differences. All three groups differed pairwise only for DPMEAN (baseline period). For the other indices, differences were only found for one or two pairs of groups.

Significant dynamics (baseline vs. heating) were shown for all indices except DPVAR in Group 3. We observed an increase in SPMAX, SPMEAN, SPVAR, DPMEAN, DPVAR (except Group 3), DP, DP/SP. The SP index was significantly decreasing.

Next, we evaluated the diagnostic informativeness of the analyzed indices in classifying patient's limbs into groups ("1" vs. "2+3") and ("1+2" vs. "3") using ROC analysis (Table 4). The evaluation was performed both for indices in the baseline period and for indices in the heating period. For the classification between "1" versus "2+3," we see that the 95% limits for AUC were above 0.5 for 11 of 15 evaluated parameters in the baseline period and for 13 of 15 evaluated parameters in the heating period.

For the classification between "1+2" versus "3," 12 out of 15 evaluated parameters had diagnostic informativeness in the baseline period and 14 out of 15 in the heating period. Thus, we see that local heating on average leads to the fact that the diagnostic informativity of pulse wave indices increases.

4 | Discussion

Changes in pulse waveforms observed by PPG have significant clinical implications. They may serve as early indicators of vascular damage in diabetes, potentially allowing earlier intervention.

Several studies have explored ways to detect DM by analyzing PPG signals, including the use of machine learning [9, 25, 26].

As a rule, changes in the pulse waveform against the background of DM are associated with an increase in the stiffness of the vascular wall, which, for example, are associated with changes in pulse wave velocity, reflection coefficient, and augmentation index [27, 28]. Most measurements are performed at rest (without the use of functional tests) [9]. The data we obtained for the baseline period are consistent with the data of the studies described above. From Groups 1 to 3, we see a significant increase in SP duration (Table 3). In Figure 4, we observe a shift of the maximum on the PPG "to the right." This also reflects the increase in vascular stiffness as the diabetic impairment intensifies.

It is known that in DM not only the structure of the vascular wall is affected, but also the regulation of vascular tone. This is associated with both endothelial dysfunction and disorders of neural regulation in DM [29]. Local heating tests are known to detect both types of these impairments. Most of these observations are shown for perfusion assessment techniques such as laser Doppler flowmetry [16, 30]. In the current work, we set out to evaluate exactly how the PPG waveform reflects changes in vascular tone during a local heating test.

Visual analysis of pulse waveform changes (Figure 4) shows that in all three groups we see a shift of the peak point to the left. This is associated with a decrease in vascular stiffness due to vasodilatation. At the same time, visually, the average shift of the maximum point (vertical dotted lines) is the same in all

TABLE 4 | Diagnostic informativeness (AUC with 95% CI) of the different indices evaluated at baseline and during the heating period.

	AUC (95% CI) for groups "1" vs. "2+3" classification		AUC (95% CI) for groups "1+2" vs. "3" classification	
	Baseline period	Heating period	Baseline period	Heating period
a_1	0.8 (0.701; 0.899) ^a	0.772 (0.671; 0.874) ^a	0.903 (0.836; 0.969) ^a	0.897 (0.799; 0.995) ^a
a_2	0.662 (0.531; 0.792) ^a	0.703 (0.588; 0.818) ^a	0.639 (0.487; 0.791)	0.653 (0.514; 0.791) ^a
a_3	0.561 (0.436; 0.687)	0.614 (0.482; 0.746)	0.776 (0.635; 0.917) ^a	0.757 (0.63; 0.884) ^a
b_1	0.743 (0.636; 0.851) ^a	0.719 (0.606; 0.832) ^a	0.759 (0.631; 0.888) ^a	0.735 (0.615; 0.855) ^a
b_2	0.714 (0.602; 0.825) ^a	0.727 (0.617; 0.837) ^a	0.803 (0.678; 0.927) ^a	0.819 (0.707; 0.932) ^a
b_3	0.656 (0.538; 0.775) ^a	0.705 (0.588; 0.823) ^a	0.805 (0.675; 0.935) ^a	0.819 (0.707; 0.931) ^a
c_2	0.636 (0.516; 0.756) ^a	0.691 (0.573; 0.81) ^a	0.812 (0.685; 0.939) ^a	0.83 (0.716; 0.944) ^a
SPMAX	0.749 (0.644; 0.854) ^a	0.76 (0.657; 0.863) ^a	0.853 (0.754; 0.953) ^a	0.892 (0.795; 0.989) ^a
SPVAR	0.652 (0.53; 0.773) ^a	0.775 (0.672; 0.878) ^a	0.804 (0.691; 0.917) ^a	0.895 (0.812; 0.979) ^a
DPMEAN	0.72 (0.61; 0.83) ^a	0.75 (0.645; 0.855) ^a	0.842 (0.739; 0.944) ^a	0.889 (0.794; 0.985) ^a
DPVAR	0.779 (0.678; 0.88) ^a	0.777 (0.677; 0.877) ^a	0.817 (0.718; 0.917) ^a	0.875 (0.789; 0.961) ^a
SPMEAN	0.549 (0.421; 0.676)	0.731 (0.616; 0.846) ^a	0.63 (0.473; 0.787)	0.783 (0.676; 0.89) ^a
SP	0.857 (0.743; 0.972) ^a	0.904 (0.815; 0.994) ^a	0.833 (0.727; 0.94) ^a	0.912 (0.837; 0.987) ^a
DP	0.497 (0.333; 0.661)	0.554 (0.39; 0.717)	0.555 (0.408; 0.701)	0.594 (0.448; 0.74)
DP/SP	0.745 (0.604; 0.886) ^a	0.819 (0.698; 0.94) ^a	0.797 (0.678; 0.915) ^a	0.862 (0.763; 0.961) ^a

^a95% CI limits for area under the curve (AUC) do not include 0.5.

three groups. We also assume that vasodilatation caused by local heating leads to a local decrease in vascular resistance to the pulse wave (due to a decrease in vascular wall tone) and, accordingly, to a faster peak on the pulse wave. It is known that both on the background of DM and with increasing age, the ability of vessels to vasodilate to local heating decreases [16], which may account for the difference in SP between the groups. We see that in Groups 2 and 3 the median SP on heating decreased by ~30 ms, and in Group 1 by ~50 ms, which may reflect the greater degree of vasodilation in Group 1 compared to Groups 2 and 3. We also see that the dicrotic notch becomes significantly more pronounced during the heating period. This effect is also evident in all three groups, but in Group 1 it is most pronounced, and in Group 3 it is least pronounced.

In all three groups, the absolute most of the indices characterizing the pulse waveform (Tables 2 and 3) underwent significant changes during the heating period in comparison with the baseline period (Wilcoxon test results marked in the tables with the symbols “+, ++, +++”). Also an important result is presented in Table 4. We see that the indices during the heating period, on average, have a higher informativeness (AUC value and the number of “significant” indices) than the assessment in the baseline period. We believe that the use of heating tests in the future may increase the informativeness of PPG technique in patients with DM.

We can identify a number of limitations in the paper. The main one is related to different age inclusion criteria in Group 1 and in Groups 2 and 3. The idea was that in Group 1 patients should not have any vascular abnormalities—neither diabetes-related nor age-related. All patients in Group 1 had comparable examinations to those in Groups 2 and 3 and the fact that they were “healthy” was confirmed by laboratory and instrumental methods. Thus, Group 1 is a model of “no disorders”, Group 2—“age-related disorders + diabetes-associated microvascular disorders”, and Group 3—“age-related disorders + diabetes-associated microvascular disorders + macrovascular disorders (lower limb arterial diseases)”. The results obtained support this hypothesis, as we see differences between Groups 2 and 3, which are comparable in age. Our future work will be devoted, among other things, to recruit age-matched groups of patients without diabetes and with early manifestations of diabetes but without complications. There is also a small imbalance of groups by gender, although it was not statistically significant. It is related to the specifics of hospitalization of patients in the departments of our clinic.

Another limitation of our study is that all subjects were Caucasian and had fair skin (second and third phototypes on the Fitzpatrick scale). However, it is known that skin tone can also affect the recorded PPG signal [31]. Thus, our results are applicable only to fair-skinned individuals.

It is also worth mentioning that we use our own heating mode to perform the functional test. We use rapid heating and assess hyperemia at about 3 min of heating. In this way, we get to the initial peak of hyperemia. Traditionally, this peak is thought to predominantly reflect “neurogenic” vasodilation, whereas endothelial mechanisms are predominantly evident in the “plateau” phase after 20–40 min of heating. However, the Minson article showed that neither inhibition of neurogenic mechanisms nor

inhibition of endothelium-dependent vasodilation leads to the disappearance of the initial hyperemic peak [18]. We conclude from this that the initial peak allows us to evaluate integrally the severity of disturbances of both “neurogenic” and “endothelial” mechanisms of vascular tone regulation.

5 | Conclusions

In the present study, we have shown that pulse waveform indices change significantly with heating in patients with DM. At the same time, some indices change comparably with the control group (e.g., shift of the maximum point), while other indices change most significantly in the control group and are less pronounced in diabetic patients (e.g., deepening of the dicrotic notch). We also showed that PPG indices during the heating period have better diagnostic characteristics than during the baseline period. We believe that the approaches we used in the current study can be used in the future to improve the informativeness of PPG studies in patients with DM.

Author Contributions

Denis Lapitan: conceptualization, formal analysis and investigation, writing – original draft preparation, writing – review and editing. **Xiaoman Xing:** formal analysis and investigation, writing – review and editing. **Alexey Glazkov:** conceptualization, methodology, formal analysis and investigation, writing – original draft preparation. **Ksenia Krasulina:** data collection. **Yulia Kovaleva:** data collection. **Polina Glazkova:** methodology. **Timur Britvin:** data collection. **Sergey Zagarov:** data collection. **Roman Larkov:** data collection. **Dmitry Rogatkin:** methodology.

Acknowledgments

The authors have nothing to report.

Ethics Statement

The study protocol complies with the ethical principles of the Declaration of Helsinki (2013 revision) and was approved by the Independent Ethics Committee of the Moscow Regional Research and Clinical Institute (“MONIKI”) (Protocol No. 13, dated November 7, 2019).

Consent

Written informed consent was obtained from all participants.

Conflicts of Interest

The authors declare no conflicts of interest.

Data Availability Statement

The data that support the findings of this study are available from the corresponding author upon reasonable request.

References

1. B. Zhou, A. W. Rayner, E. W. Gregg, et al., “Worldwide Trends in Diabetes Prevalence and Treatment From 1990 to 2022: A Pooled Analysis of 1108 Population-Representative Studies With 141 Million Participants,” *Lancet* 404 (2024): 2077–2093, [https://doi.org/10.1016/S0140-6736\(24\)02317-1](https://doi.org/10.1016/S0140-6736(24)02317-1).

2. Y.-K. Jan, N. Kelhofer, T. Tu, et al., "Diagnosis, Pathophysiology and Management of Microvascular Dysfunction in Diabetes Mellitus," *Diagnostics* 14, no. 24 (2024): 2830, <https://doi.org/10.3390/diagnostic14242830>.
3. D. A. Kulikov, A. A. Glazkov, Y. A. Kovaleva, N. V. Balashova, and A. V. Kulikov, "Prospects of Laser Doppler Flowmetry Application in Assessment of Skin Microcirculation in Diabetes," *Diabetes Mellitus* 20 (2017): 279–285, <https://doi.org/10.14341/DM8014-6906>.
4. E. Zharkikh, V. Dremin, E. Zherebtsov, A. Dunaev, and I. Meglinski, "Biophotonics Methods for Functional Monitoring of Complications of Diabetes Mellitus," *Journal of Biophotonics* 13 (2020): e202000203, <https://doi.org/10.1002/jbio.202000203>.
5. A. Glazkov, K. Krasulina, P. Glazkova, et al., "Detection of Cutaneous Blood Flow Changes Associated With Diabetic Microangiopathies in Type 2 Diabetes Patients Using Incoherent Optical Fluctuation Flowmetry," *Photonics* 10 (2023): 442, <https://doi.org/10.3390/photonics10040442>.
6. J. Allen, "Photoplethysmography and Its Application in Clinical Physiological Measurement," *Physiological Measurement* 28 (2007): R1–R39, <https://doi.org/10.1088/0967-3334/28/3/R01>.
7. M. Elgendi, "On the Analysis of Fingertip Photoplethysmogram Signals," *Current Cardiology Reviews* 8 (2012): 14–25, <https://doi.org/10.2174/157340312801215782>.
8. E. von Wowern, G. Östling, P. M. Nilsson, and P. Olofsson, "Digital Photoplethysmography for Assessment of Arterial Stiffness: Repeatability and Comparison With Applanation Tonometry," *PLoS One* 10 (2015): e0135659, <https://doi.org/10.1371/journal.pone.0135659>.
9. S. Zanelli, M. Ammi, M. Hallab, and M. A. El Yacoubi, "Diabetes Detection and Management Through Photoplethysmographic and Electrocardiographic Signals Analysis: A Systematic Review," *Sensors* 22 (2022): 4890, <https://doi.org/10.3390/s22134890>.
10. K. Pilt, K. Meigas, R. Ferenets, K. Temitski, and M. Viigimaa, "Photoplethysmographic Signal Waveform Index for Detection of Increased Arterial Stiffness," *Physiological Measurement* 35 (2014): 2027–2036, <https://doi.org/10.1088/0967-3334/35/10/2027>.
11. V. R. Reddy, A. D. Choudhury, P. Deshpande, S. Jayaraman, N. K. Thokala, and V. Kaliaperumal, "DMSense: A Non-Invasive Diabetes Mellitus Classification System Using Photoplethysmogram Signal," in *2017 IEEE International Conference on Pervasive Computing and Communications Workshops (PerCom Workshops)* (IEEE, 2017), 71–73, <https://doi.org/10.1109/PERCOMW.2017.7917526>.
12. N. Nirala, R. Periyasamy, B. K. Singh, and A. Kumar, "Detection of Type-2 Diabetes Using Characteristics of Toe Photoplethysmogram by Applying Support Vector Machine," *Biocybernetics and Biomedical Engineering* 39 (2019): 38–51, <https://doi.org/10.1016/j.bbe.2018.09.007>.
13. M. Roustit, F. Maggi, S. Isnard, M. Hellmann, B. Bakken, and J. L. Cracowski, "Reproducibility of a Local Cooling Test to Assess Microvascular Function in Human Skin," *Microvascular Research* 79 (2010): 34–39, <https://doi.org/10.1016/j.mvr.2009.11.004>.
14. D. G. Lapitan and D. A. Rogatkin, "Functional Studies on Blood Microcirculation System With Laser Doppler Flowmetry in Clinical Medicine: Problems and Prospects," *Almanac of Clinical Medicine* 44, no. 2 (2016): 249–259, <https://doi.org/10.18786/2072-0505-2016-44-2-249-259>.
15. A. Kamshilin, A. Belaventseva, R. Romashko, Y. N. Kulchin, and O. V. Mamontov, "Local Thermal Impact on Microcirculation Assessed by Imaging Photoplethysmography," *Biology and Medicine* 8 (2016): 361, <https://doi.org/10.4172/0974-8369.1000361>.
16. D. Fuchs, P. P. Dupon, L. A. Schaap, and R. Draijer, "The Association Between Diabetes and Dermal Microvascular Dysfunction Non-Invasively Assessed by Laser Doppler With Local Thermal Hyperemia: A Systematic Review With Meta-Analysis," *Cardiovascular Diabetology* 16 (2017): 1–12, <https://doi.org/10.1186/s12933-016-0487-1>.
17. I. Mizeva, E. Zharkikh, V. Dremin, et al., "Spectral Analysis of the Blood Flow in the Foot Microvascular Bed During Thermal Testing in Patients With Diabetes Mellitus," *Microvascular Research* 120 (2018): 13–20, <https://doi.org/10.1016/j.mvr.2018.05.005>.
18. C. T. Minson, L. T. Berry, and M. J. Joyner, "Nitric Oxide and Neuromodulatory Regulation of Skin Blood Flow During Local Heating," *Journal of Applied Physiology* 91 (2001): 1619–1626, <https://doi.org/10.1152/jappl.2001.91.4.1619>.
19. M. Roustit, S. Blaise, C. Millet, and J. L. Cracowski, "Reproducibility and Methodological Issues of Skin Post-Occlusive and Thermal Hyperemia Assessed by Single-Point Laser Doppler Flowmetry," *Microvascular Research* 79 (2010): 102–108, <https://doi.org/10.1016/j.mvr.2010.01.001>.
20. P. Glazkova, A. Glazkov, D. Kulikov, et al., "Incoherent Optical Fluctuation Flowmetry for Detecting Limbs With Hemodynamically Significant Stenoses in Patients With Type 2 Diabetes," *Endocrine* 82 (2023): 550–559, <https://doi.org/10.1007/s12020-023-03506-4>.
21. R. Couceiro, P. de Carvalho, R. P. Paiva, et al., "Assessment of Cardiovascular Function From Multi-Gaussian Fitting of a Finger Photoplethysmogram," *Physiological Measurement* 36, no. 9 (2015): 1801–1825, <https://doi.org/10.1088/0967-3334/36/9/1801>.
22. M. C. Baruch, D. E. Warburton, S. S. Bredin, A. Cote, D. W. Gerdt, and C. M. Adkins, "Pulse Decomposition Analysis of the Digital Arterial Pulse During Hemorrhage Simulation," *Nonlinear Biomedical Physics* 5, no. 1 (2011): 1–15, <https://doi.org/10.1186/1753-4631-5-1>.
23. X. Xing, Z. Ma, M. Zhang, et al., "Robust Blood Pressure Estimation From Finger Photoplethysmography Using Age-Dependent Linear Models," *Physiological Measurement* 41 (2020): 025007, <https://doi.org/10.1088/1361-6579/ab755d>.
24. D. G. Lapitan, A. A. Glazkov, and D. A. Rogatkin, "Evaluation of the Age-Related Changes of Elasticity of Peripheral Vascular Walls by Photoplethysmography," *Meditinskaya Fizika* 87 (2020): 71–77.
25. P.-C. Hsu, H.-T. Wu, and C.-K. Sun, "Assessment of Subtle Changes in Diabetes-Associated Arteriosclerosis Using Photoplethysmographic Pulse Wave From Index Finger," *Journal of Medical Systems* 42 (2018): 43, <https://doi.org/10.1007/s10916-018-0901-1>.
26. S. Usman, N. Bani, M. H. Kaidi, S. A. M. Aris, S. Z. A. Jalil, and M. N. Muhtazaruddin, "Second Derivative and Contour Analysis of PPG for Diabetic Patients," in *2018 IEEE-EMBS Conference on Biomedical Engineering and Sciences (IECBES)* (IEEE, 2018), 59–62, <https://doi.org/10.1109/IECBES.2018.8626681>.
27. M. Zhang, Y. Bai, P. Ye, et al., "Type 2 Diabetes Is Associated With Increased Pulse Wave Velocity Measured at Different Sites of the Arterial System but Not Augmentation Index in a Chinese Population," *Clinical Cardiology* 34 (2011): 622–627, <https://doi.org/10.1002/clc.20956>.
28. H. Gunathilaka, R. Rajapaksha, T. Kumarika, et al., "Non-Invasive Diagnostic Approach for Diabetes Using Pulse Wave Analysis and Deep Learning," *Informatics* 11 (2024): 51, <https://doi.org/10.3390/informatics11030051>.
29. J.-L. Cracowski and M. Roustit, "Local Thermal Hyperemia as a Tool to Investigate Human Skin Microcirculation," *Microcirculation* 17 (2010): 79–80, <https://doi.org/10.1111/j.1549-8719.2009.00018.x>.
30. Z. Stoyneva, I. Velcheva, N. Antonova, and E. Titanova, "Microvascular Reactivity to Thermal Stimulation in Patients With Diabetes Mellitus and Polyneuropathy," *Clinical Hemorheology and Microcirculation* 65 (2017): 67–75, <https://doi.org/10.3233/CH-15107>.
31. B.-A. T. Ajmal, A. J. Rodriguez, V. N. Du Le, and J. C. Ramella-Roman, "Monte Carlo Analysis of Optical Heart Rate Sensors in Commercial Wearables: The Effect of Skin Tone and Obesity on the Photoplethysmography (PPG) Signal," *Biomedical Optics Express* 12 (2021): 7445–7457, <https://doi.org/10.1364/BOE.439893>.